Solar Phys (2010) 267: 267–277
DOI 10.1007/s11207-010-9653-x

# Solar Polar Fields During Cycles 21 – 23: Correlation with Meridional Flows

**P. Janardhan · Susanta K. Bisoi · S. Gosain**

Received: 16 April 2010 / Accepted: 29 September 2010 / Published online: 2 November 2010


**Abstract** We have examined polar magnetic fields for the last three solar cycles, *viz*. Cycles 21, 22, and 23 using NSO/Kitt Peak synoptic magnetograms. In addition, we have used SOHO/MDI magnetograms to derive the polar fields during Cycle 23. Both Kitt Peak and MDI data at high latitudes (78° – 90°) in both solar hemispheres show a significant drop in the absolute value of polar fields from the late declining phase of the Solar Cycle 22 to the maximum of the Solar Cycle 23. We find that long-term changes in the absolute value of the polar field, in Cycle 23, are well correlated with changes in meridional-flow speeds that have been reported recently. We discuss the implication of this in influencing the extremely prolonged minimum experienced at the start of the current Cycle 24 and in forecasting the behavior of future solar cycles.

**Keywords** Polar magnetic fields · Meridional flows · Solar cycle · MDI magnetograms

## 1. Introduction

Detailed study of solar magnetic features is an important area of research not only for its intrinsic interest, but also because solar magnetic fields have a profound and far-reaching influence on the Earth's near-space environment. With society's increased dependence on space-based technology, much of which is at risk due to solar activity that waxes and wanes

P. Janardhan (✉) · S.K. Bisoi · S. Gosain
Physical Research Laboratory, Astronomy & Astrophysics Division, Navrangpura, Ahmedabad 380009, India
e-mail: jerry@prl.res.in

S.K. Bisoi
e-mail: susanta@prl.res.in

S. Gosain
e-mail: sgosain@prl.res.in

S. Gosain
Udaipur Solar Observatory, P.O. Box 198, Dewali, Udaipur 313001, India

with the sunspot cycle, it is imperative that we understand the solar magnetic cycle and its effects on the near-space environment. In addition, due to the reported anthropogenic influence on climate change that has occurred in recent times, it is becoming increasingly important to distinguish and delineate the degree to which the solar cycle can affect terrestrial climate.

The evolution of the large-scale solar magnetic field is attributed to a solar magnetohydrodynamic dynamo operating inside the Sun which involves three basic processes. The generation of toroidal fields by shearing pre-existing poloidal fields (the $\Omega$ effect), the regeneration of poloidal fields by twisting toroidal flux tubes (the $\alpha$ effect), and finally, flux transport by meridional circulation to carry background magnetic fields polewards from the Equator (Parker, 1955a, 1955b; Steenbeck and Krause, 1969; Wang, Sheeley, and Nash, 1991; Choudhuri, Schussler, and Dikpati, 1995; Dikpati and Charbonneau, 1999) are considered.

With the measurement of the Sun's polar field (Babcock and Babcock, 1955) and the subsequent proposal of polar-field reversal during the maximum of each solar cycle (Babcock, 1959), research on solar magnetic fields and their effect on subsequent cycles was channelled in a new direction. Since then, many investigations have been carried out to explore the relation between evolution of large-scale magnetic fields and their association with polar-field structures (Fox, McIntosh, and Wilson, 1998; Benevolenskaya, Kosovichev, and Scherrer, 2001; Benevolenskaya, Kosovichev, and Scherrer, 2002; Gopalswamy *et al.*, 2003).

The current sunspot minimum, which we have seen at the end of Cycle 23, has been one of the deepest minima that we have experienced in recent times with roughly 71–73% of the days in 2008 and 2009, respectively, being entirely spotless. Apart from this, Cycle 23 has shown several other peculiarities, such as a second maximum during the declining phase that is unusual for odd-numbered cycles, a slower rise to maximum than other odd-numbered cycles, and a slower than average polar reversal. Such departures from "normal" behavior need to be studied and understood as they could be significant in the context of understanding the evolution of magnetic fields on the Sun.

In this article, we have examined the solar polar-field behavior for the last few cycles and the following sections will discuss our findings.

## 2. Magnetic-Field Data

### 2.1. Low-resolution NSO/Kitt Peak Data

Magnetic-field data are available as standard FITS format files from the National Solar Observatory, Kitt Peak, USA (NSO/Kitt Peak) synoptic magnetogram database (ftp://nsokp.nso.edu/kpvt/synoptic/mag/). These synoptic maps are in the form of $180\times360$ arrays starting from Carrington Rotation (CR) CR1625 through CR2006 corresponding to years 1975.13 through 2003.66. For the period covering the years from 2003.66 through 2009.11, synoptic maps were obtained from the *Vector Spectro Magnetograph* (VSM) of the NSO/*Synoptic Optical Long-term Investigations of the Sun* (SOLIS) facility for solar observations over a long time frame (NSO/SOLIS): (ftp://solis.nso.edu/synoptic/level3/vsm/merged/carr-rot/). A few data gaps during CR1640 – CR1644, CR1854, CR1890, CR2015, CR2016, CR2040, and CR2041 were filled in by interpolated values while making the plots.

The resolution of the synoptic maps is 1° in both longitude (1° to 360°) and latitude (−90° to 90°). A typical Carrington synoptic map is produced from full-disk magnetograms spanning an entire Carrington rotation period. Each individual magnetogram is first remapped into latitude and longitude coordinates and then added together to produce

the final synoptic map for each CR. All synoptic magnetogram maps, represented as an $i \times j$ data array with $i$ and $j$ representing the latitude and longitude respectively, for any given CR number $n$, contain magnetic flux density $[\phi_{i,j,n}]$, in units of Gauss averaged over equal areas of the Sun. The actual flux units are then obtained by multiplying by the appropriate area.

Since we are interested in the variation of photospheric magnetic fields with latitude, data are processed by taking longitudinal averages for each latitude bin of 1° by converting the data to a one dimensional array of $180 \times 1$. Any latitude element $i$, for a given CR, $[n]$ will contain the averaged magnetic field represented by Equation (1),

$$\phi_{i,n} = \frac{\sum_{j=1}^{360} \phi_{i,j,n}}{360} \tag{1}$$

Now, the averaged magnetic field for a range of latitudes in any CR is obtained by averaging $\phi_{i,n}$, as shown by Equation (2),

$$\phi_n = \frac{\sum_{i=k}^{p} \phi_{i,n}}{p - k + 1} \tag{2}$$

Here $k$ and $p$ are the row numbers corresponding to a latitude bin. Using the above procedure, we have obtained average magnetic fields in each solar hemisphere for three different latitude bins between ranges:

- 0° and 45°, representing the equatorial or toroidal fields.
- 45° and 78°, representing the mid-latitude fields.
- 78° and 90°, representing polar fields in each hemisphere.

### 2.2. High-Resolution MDI Data

Line-of-sight magnetograms from the *Michelson Doppler Interferometer* (MDI: Scherrer *et al.*, 1995), onboard the *Solar and Heliospheric Observatory* (SOHO: Domingo, Fleck, and Poland, 1995), are available from 1996 onwards. High-resolution ($3600 \times 1080$ pixels) MDI synoptic images beginning from CR1911 through CR2080 are used, with data gaps for CR1938 – CR1942, CR1945, and CR2073. It must, however, be noted that there are occasions that the inclination of the Earth's orbit to the Sun's Equator will cause one of the poles of the Sun to not be clearly visible. We have used MDI synoptic magnetograms available at http://soi.stanford.edu/magnetic/index6.html, which have been corrected for this effect.

Since MDI measurements are considered to be more reliable, as they are more frequent and stable as compared to Kitt Peak observations, we have compared the two data sets for the period after 1996 to check if the results agree with each other. Also, data gaps, when present, for example from CR1938 to CR1941, were dealt with by replacing them with interpolated values, and these have been indicated in the figures. Finally, the resolution of the MDI data was degraded (by averaging) to the resolution of the NSO/Kitt Peak data so as to be able to compare the results. It may be noted that for the MDI data, only the latitude bin between 78° and 90° was considered.

## 3. Magnetic-Field Measurements

As mentioned earlier, meridional circulation is the primary poloidal-flux-transport agent in the Sun. A polewards meridional flow at the solar surface has been shown to exist,

with average speeds in the range 10 $\mathrm{m\,s^{-1}}$ – 20 $\mathrm{m\,s^{-1}}$ (Duvall, 1979; Hathaway, 1996; Hathaway *et al.*, 1996). The amplitude of this surface flow is more than an order of magnitude weaker than other surface flows, such as granulation, supergranulation and differential rotation. Therefore, the effects of this meridional circulation can best be studied at high solar latitudes, where the modulation due to the solar cycle is negligible or absent.

Figure 1 shows the measurements of the magnetic field in each solar hemisphere as a function of time in the two latitude ranges 0° – 45° and 45° – 78°. While the upper two panels of Figure 1 show the absolute value of the field in the latitude range 0° – 45° for the northern and southern hemisphere, respectively, the lower two panels show the absolute value of the magnetic field in the latitude range 45° – 78° for the northern and southern hemisphere, respectively. The filled dots represent the actual measurements derived from the NSO/Kitt Peak data base, while the solid line is a smoothed curve representing the data. The vertically oriented dashed parallel lines demarcate Cycles 21, 22, and 23. It can be seen from Figure 1 (upper two panels) that there is a strong solar-cycle modulation present in the latitude range ±0° – ±45°, while the solar-cycle modulation is much weaker and barely discernable in the latitude range ±45° – ±78° for Cycles 21 and 22; it is not seen for Cycle 23.

Figure 2 shows the actual (signed) measurements of magnetic field, in each solar hemisphere, as a function of time in years in the latitude range 78° – 90°. While the upper panel of Figure 2 shows the magnetic field for the northern hemisphere, the lower panel shows the value of the magnetic field for the southern hemisphere. The filled dots, with $1\sigma$ error bars, represent the measurements derived from the NSO/Kitt Peak data, while the thick, solid, blue line is a smoothed curve. Points where data gaps were filled by interpolation are shown by red open circles. A comparison of the polar field during Cycles 22 and 23 from Figure 2 shows that the longitude-averaged polar magnetic field between ±78° – ±90° during the current extended minimum leading up to the current Cycle 24 is weaker than the corresponding minimum period in Cycles 21 and 22. Also, a comparison of the fields in the two hemispheres in Cycle 23 shows that the south polar field is weaker than the north polar field. In a detailed analysis of sunspot data and longitude-averaged photospheric magnetic flux, Dikpati *et al.* (2004) have also pointed out several peculiarities during Cycle 23 such as the slow buildup of the polar field after the occurrence of the polar-field reversal, the asymmetry in polar reversal for the North and South Pole, and the steady behavior of the north polar field in comparison to the south polar field from the late declining phase of Cycle 22 to early rising phase of Cycle 23. All of these features can also clearly be seen in Figure 2 for the period of Cycle 23.

The two panels of Figure 3 show the variation in the absolute value of the polar magnetic field in the latitude range 78° – 90° for the north and south solar hemisphere as a function of years for Solar Cycles 21 – 23. Measurements from NSO/Kitt Peak data are shown by filled dots, while the thick, blue, solid line is a smoothed curve. During Cycle 23, MDI data are shown by red crosses to enable comparison between NSO/Kitt Peak data and MDI data. Marked by open black circles are points where MDI data gaps were filled in by interpolation. It may be noted that the MDI high-resolution data were reduced, by averaging, to that of the NSO/Kitt Peak data for comparison. A striking feature in Figure 3 is a steep and continuous drop of the average polar field (in both NSO and MDI data) from the late declining phase of Cycle 22 to the maximum of Cycle 23 in both the hemispheres. A slow continuous drop of $\approx$ 13 G from 1994 to 2001 is seen in the northern hemisphere, while a sharp continuous drop of $\approx$ 9 G from 1995 to 2002 is seen in the southern hemisphere. Cycles 21 and 22, however, showed no such drop. The recent and extended minimum at the end of Cycle 23 is also interesting in that the average polar-field behavior showed no variation and remained steady from 2004 onwards in both hemispheres as seen from both NSO and MDI data. The MDI data however, are systematically lower than the NSO/Kitt Peak values throughout Cycle 23.

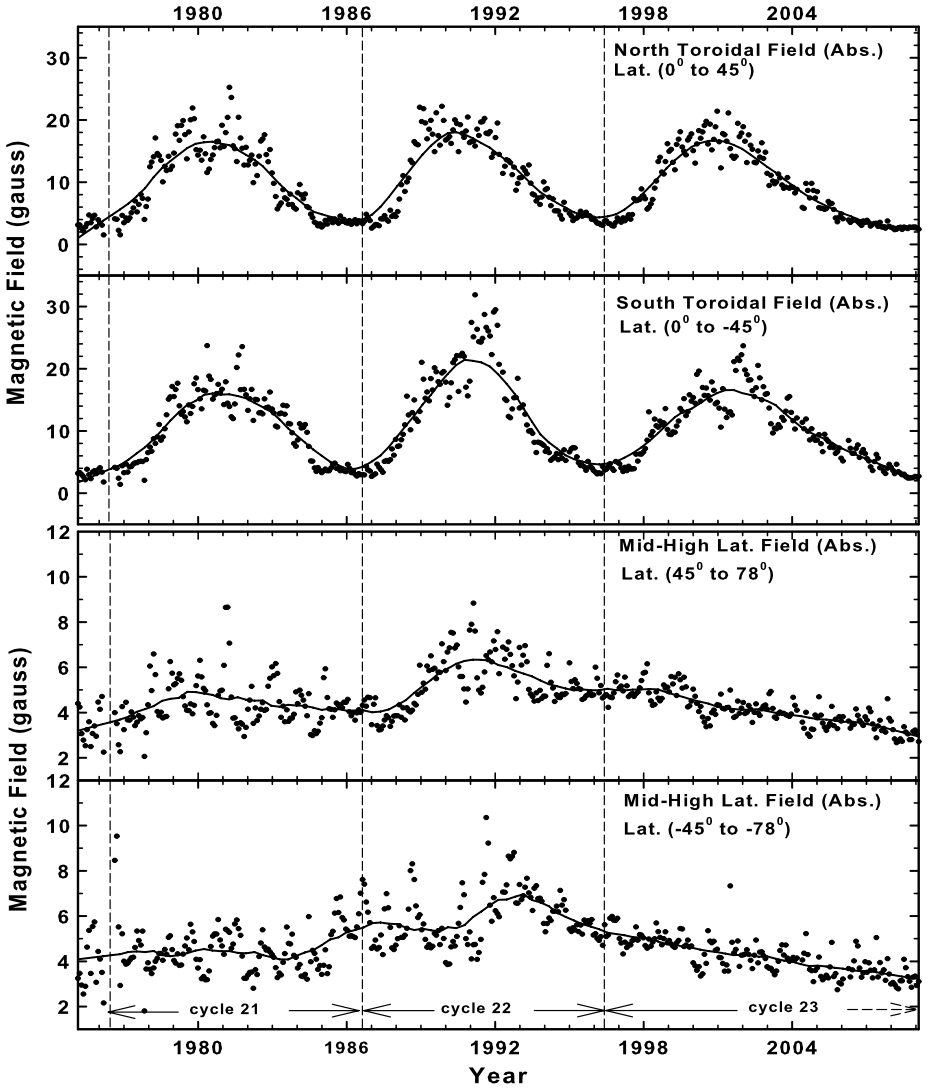


**Figure 1** The four panels, in pairs starting from the top, show the variations in the magnetic field in the north and south solar hemisphere respectively, as a function of years for Solar Cycles 21 – 23. The absolute value of the magnetic field in the latitude range $0° - \pm 45°$ is shown in the first pair of panels, while the second pair of panels show the absolute value of magnetic field in the latitude range $45° - 78°$. The filled dots represent the actual measurements, while the solid line is a smoothed curve. The vertically oriented dashed parallel lines demarcate Cycles 21, 22, and 23, respectively.

## 4. Polar Fields and Meridional-Flow Speeds

### 4.1. Cycle 23

The Sun's meridional flow, which is directed polewards at the surface of the Sun, is an axis-symmetric flow of the order of $10 - 20\ \mathrm{m\,s^{-1}}$. This meridional flow is responsible for carrying background magnetic fields polewards from the Equator and plays an important

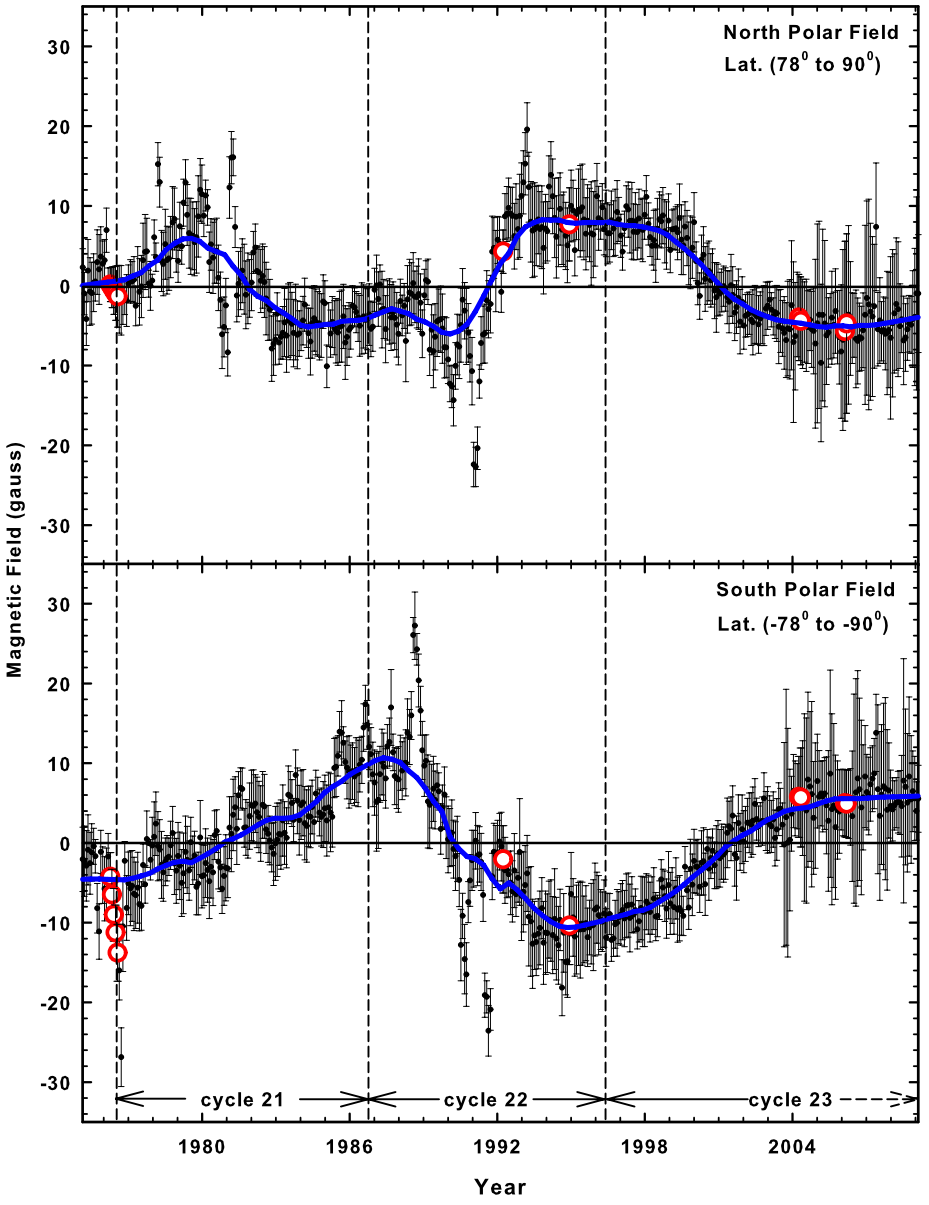


**Figure 2** Variations in the magnetic field in the northern (upper panel) and southern solar hemisphere (lower panel) as a function of years for Solar Cycles 21 – 23. The actual (signed) value of magnetic field in the latitude range 78° – 90° is shown (filled dots) with 1$\sigma$ error bars, while the thick, blue, solid line is a smoothed curve. The vertically oriented, dashed, parallel lines demarcate Cycles 21, 22, and 23, respectively. Points where data gaps were filled by interpolation are shown by red open circles

role in determining the strength of the solar polar field and the intensity of sunspot cycles (see, *e.g.*, Hathaway and Rightmire, 2010). There have been some attempts to infer surface meridional-flow speeds using the helioseismic technique of ring-diagram analysis applied

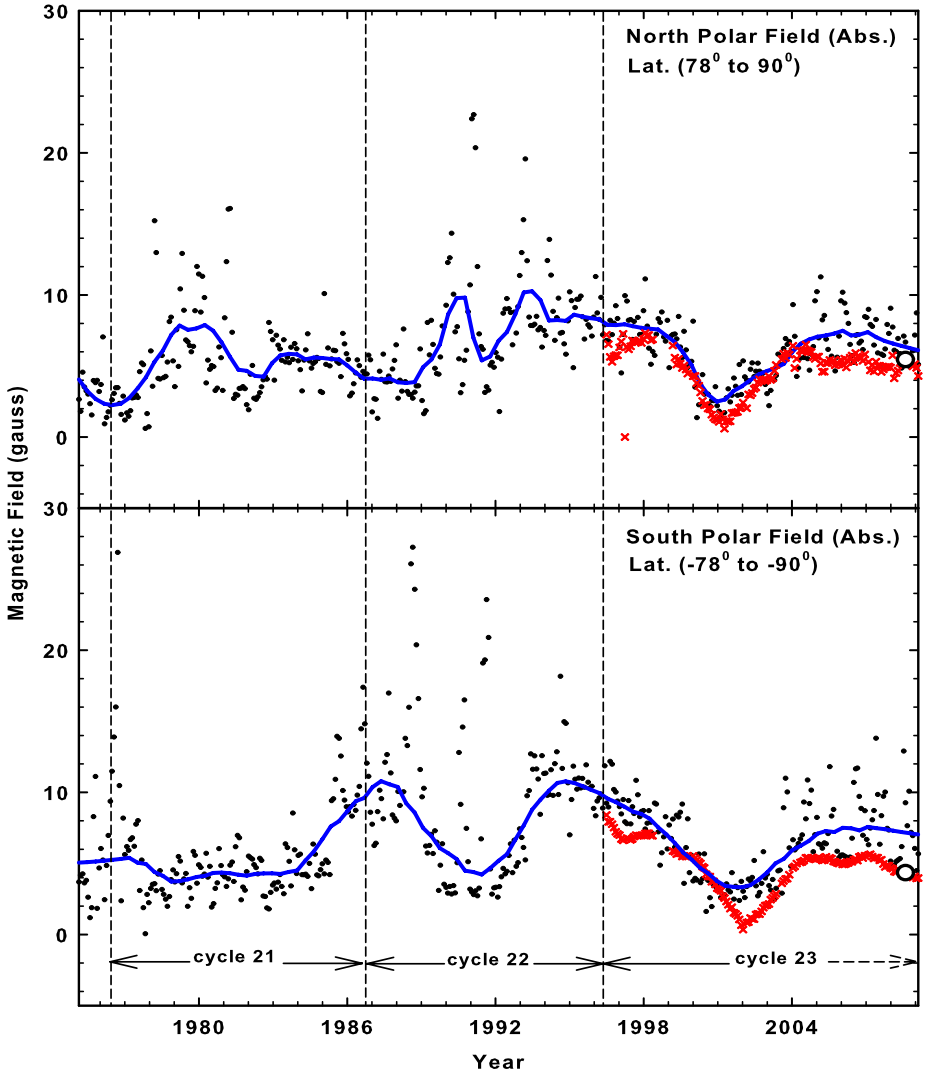


**Figure 3** Variations in the absolute value of the polar magnetic field in the latitude range 78° – 90° for the north and south solar hemisphere as a function of years for the Solar Cycles 21 – 23. The measurements derived from the NSO/Kitt Peak data base are shown by filled dots, while the thick, blue, solid line is a smoothed curve. MDI data for Cycle 23 (for comparison) are shown by red crosses. The vertically oriented, dashed, parallel lines demarcate Cycles 21, 22, and 23 respectively. Points where MDI data gaps were filled by interpolation are shown by black open circles.

to MDI data (Haber *et al.*, 2002). However, a more recent and detailed study using MDI images of the line-of-sight magnetic fields (Hathaway and Rightmire, 2010) has reported measurements of the surface meridional-flow speed in the latitude range ±75° in Cycle 23. These measurements have shown a lot of variation in the meridional-flow speeds in Cycle 23. These authors determined a meridional-flow speed of 11.5 m s$^{-1}$ at the minimum of Cycle 23 in 1996 – 1997 which then dropped to 8.5 m s$^{-1}$ at the maximum in 2000 – 2001. It must be noted here that this drop in the flow speed coincides with the steep drop in the absolute

value of the magnetic field that is seen in both the NSO/Kitt Peak and MDI data (Figure 3). In fact, the MDI data in the southern hemisphere continue to drop until 2002, after which they rise again. Between 2001 and 2004, the measured meridional-flow speed again increased to 13.0 m $s^{-1}$ and remained constant at this value thereafter. Again, from Figure 3 we can see a corresponding steep increase in the absolute value of the polar field between 2001 and 2004. After this, the absolute value of the magnetic field remains constant in both hemispheres until 2009. From Figure 3 it is clear that the polar-field strength since 2004, as seen by both NSO/Kitt Peak and MDI has remained constant. Figure 4 shows a comparison between the averaged absolute magnetic fields determined from NSO/Kitt Peak synoptic magnetogram maps and MDI synoptic magnetogram maps for the northern (upper panel) and southern (lower panel) hemispheres for Solar Cycle 23. While the solid line is a smoothed curve representing the NSO data, the dashed line is a smoothed curve representing the MDI data. The meridional-flow speeds, as reported by Hathaway and Rightmire (2010), are indicated at the bottom of each panel and demarcated by vertically oriented, dashed parallel lines. It may be noted again that the MDI high-resolution data ($3600\times1080$ pixels) were averaged and reduced to that of the NSO/Kitt Peak data ($360\times180$ pixels) for comparison. The recent and extended minimum at the end of Cycle 23 is also interesting in that the average polar-field behavior showed no variation and remained steady from 2004 onwards in both hemispheres as seen from Figure 4. The magnetic field of MDI data, however, are systematically lower than the NSO/Kitt Peak values throughout Cycle 23, and in the southern hemisphere, the MDI data show a steep drop between 1997 – 2002.

### 4.2. Strength of Upcoming Solar Cycle 24

In trying to predict the strength of future solar cycles, magnetic persistence or the Sun's memory of the polar-field strength at minimum in the previous cycle has been postulated as the influencing factor. Some authors have used this method to try and predict the strength of upcoming cycles through magnetic persistence or the Sun's memory (Schatten *et al.*, 1978; Layden *et al.*, 1991; Schatten and Sofia, 1996). Later, it was postulated that magnetic persistence is itself governed by the meridional-flow speed (Hathaway, 1996; Haber *et al.*, 2002; Basu and Antia, 2003) with slower meridional flows resulting in longer memory. In addition, a slower meridional-flow speed would also determine the cycle period.

Two different views were postulated to predict the strength of Solar Cycle 24. The first predicted the new Solar Cycle 24 to be a strong cycle compared to Cycle 23 (Dikpati, de Toma, and Gilman, 2006). These authors used the sunspot area of the last three cycles based on a flux-transport-dynamo model as the source term for generating the poloidal field. The second predicted the new Solar Cycle 24 to be a weak one (Choudhuri, Chatterjee, and Jiang, 2007). These authors used only inputs from the last solar cycle, since the generation of poloidal fields involved randomness and indeterministic behavior.

### 4.3. Discussion and Conclusions

Although a great deal of progress has been made in our understanding of meridional flows and their role in determining the strength of the polar field and the amplitude of the following cycles, there seems to be a basic disagreement between flux-transport-dynamo models and surface-flux-transport models. Fast meridional flows, in the flux-transport-dynamo models, produce stronger polar fields and a short cycle, as compared to the observations of surface-flux-transport model, which give rise to weak polar fields and a long solar cycle. While the dynamo models have fields of one polarity centred on the sunspot latitudes, surface-flux-transport models have bands of opposite magnetic polarity on either side of the sunspot

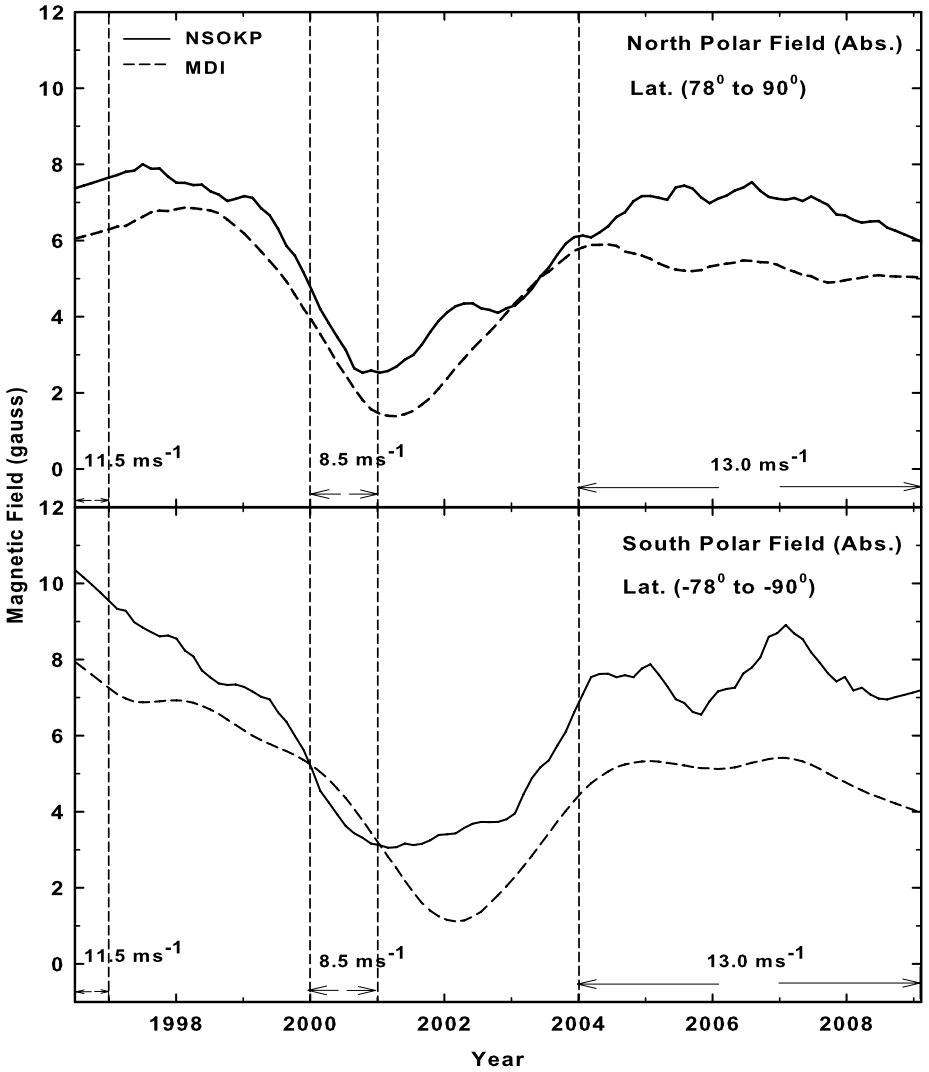


**Figure 4** Comparison between Kitt Peak/NSO data and MDI data in Cycle 23 for the two hemispheres. The northern hemisphere is shown in the upper panel, while the southern hemisphere is shown in the lower panel. The meridional-flow speeds as reported by Hathaway and Rightmire (2010) have been indicated between vertically oriented dashed parallel lines.

latitudes. The cause for the difference in these two models is mainly the above difference in the latitudinal distribution of magnetic polarities, and this has been explained by Hathaway and Rightmire (2010); see also the references therein.

The observations of Hathaway and Rightmire (2010) support the surface-flux-transport model, wherein fast meridional flows inhibit opposite polarities from cancelling each other across the Equator. Thus, elements of both polarities will be carried to the poles, and a longer time would be required to reverse the old polar fields. This would in turn result in weaker polar fields of the new or reversed polarity. Such a mechanism would support our observa-

tions of weaker polar fields at solar maximum. We have seen from our data that we have a large and unusual drop in the absolute value of the polar fields during Cycle 23 compared to previous cycles (Section 3) and we also see its association with a similar behavior in the meridional-flow speed (Section 4.1). In addition, Hathaway and Rightmire (2010) have shown that the meridional flow generally shows a decrease from minimum to maximum, as has also been reported for earlier solar cycles (Komm, Howard, and Harvey, 1993), although with greater uncertainty and poorer temporal resolution than for Cycle 23, where high-resolution MDI data are available. The minimum leading up to the start of Cycle 24 has been very deep and prolonged, and we have seen that the corresponding polar fields have been at their lowest compared to Cycles 21 and 22. We believe that the "memory" of this very weak polar field in Cycle 23 is the cause of the extended solar minimum we have witnessed. Since the Sun's memory depends on the polar-field strength we believe that the upcoming Cycle 24 will be a much weaker cycle than Cycle 23, which is in accordance with the later prediction proposed by Choudhuri, Chatterjee, and Jiang (2007).

We have seen above that the absolute value of the polar magnetic field in the latitude range $78^\circ - 90^\circ$ virtually mirrors the change in the meridional-flow speeds in Cycle 23, with meridional-flow speeds dropping when the absolute value of the field drops. Unlike Cycles 21 and 22, the absolute values of the polar magnetic fields in Cycle 23 showed similar trends in both hemispheres. Since high-resolution MDI data are available only from 1996, this approach cannot be used to compute meridional flows for Cycles 21 and 22 noted that in both Cycles 21 and 23 the behavior of the absolute value of the polar fields is different in each hemisphere. If we assume that the correlation between the absolute value of the polar fields and the meridional-flow velocities holds good for all solar cycles, then this would imply that the field reversals occurred at different times in the two hemispheres in Cycles 21, 22, and 23.

The study of polar magnetic fields might thus provide good clues to the nature of the meridional flows in each hemisphere. Such inputs would be important in predicting the behavior of the future solar cycles. In addition to such measurements, other inputs from radio measurements of circular polarization that are sensitive to the line-of-sight component of the coronal magnetic field will also be very useful. The same is true for interplanetary scintillation measurements at high latitudes that can indicate the change in turbulence levels due to changes in polar fields (Ananthakrishnan, Balasubramanian, and Janardhan, 1995). Finally, high-resolution high-dynamic-range quiet-Sun radio imaging (Mercier *et al.*, 2006) of the Sun at low frequencies that can examine the changes in polar coronal-hole boundaries may be useful.

**Acknowledgements** The authors are thankful for the free-use data policy of the National Solar Observatory and acknowledge the MDI consortium for providing the data in the public domain via the world wide web. SOHO is a project of international collaboration between ESA and NASA. One of the authors (JP) would like to thank Murray Dryer for his critical comments on the manuscript.

## References

Ananthakrishnan, S., Balasubramanian, V., Janardhan, P.: 1995, Latitudinal variation of solar wind velocity. *Space Sci. Rev.* **72**, 229 – 232. doi:10.1007/BF00768784.

Babcock, H.D.: 1959, The Sun's polar magnetic field. *Astrophys. J.* **130**, 364. doi:10.1086/146726.

Babcock, H.W., Babcock, H.D.: 1955, The sun's magnetic field, 1952 – 1954. *Astrophys. J.* **121**, 349. doi:10.1086/145994.

Basu, S., Antia, H.M.: 2003, Changes in solar dynamics from 1995 to 2002. *Astrophys. J.* **585**, 553 – 565. doi:10.1086/346020.

Benevolenskaya, E.E., Kosovichev, A.G., Scherrer, P.H.: 2001, Detection of high-latitude waves of solar coronal activity in extreme-ultraviolet data from the Solar and Heliospheric Observatory EUV Imaging Telescope. *Astrophys. J. Lett.* **554**, L107 – L110. doi:10.1086/320925.

Benevolenskaya, E.E., Kosovichev, A.G., Scherrer, P.H.: 2002, Evolution of large-scale coronal structure with the solar cycle from EUV data. In: Favata, F., Drake, J.J. (eds.) *Stellar Coronae in the Chandra and XMM-NEWTON Era* **CS-277**, Astron. Soc. Pac., San Fransisco, 419.

Choudhuri, A.R., Schussler, M., Dikpati, M.: 1995, The solar dynamo with meridional circulation. *Astron. Astrophys.* **303**, L29.

Choudhuri, A.R., Chatterjee, P., Jiang, J.: 2007, Predicting solar cycle 24 with a solar dynamo model. *Phys. Rev. Lett.* **98**(13), 131103. doi:10.1103/PhysRevLett.98.131103.

Dikpati, M., Charbonneau, P.: 1999, A Babcock – Leighton flux transport dynamo with solar-like differential rotation. *Astrophys. J.* **518**, 508 – 520. doi:10.1086/307269.

Dikpati, M., de Toma, G., Gilman, P.A.: 2006, Predicting the strength of solar cycle 24 using a flux-transport dynamo-based tool. *Geophys. Res. Lett.* **33**, 5102. doi:10.1029/2005GL025221.

Dikpati, M., de Toma, G., Gilman, P.A., Arge, C.N., White, O.R.: 2004, Diagnostics of polar field reversal in solar cycle 23 using a flux transport dynamo model. *Astrophys. J.* **601**, 1136 – 1151. doi:10.1086/380508.

Domingo, V., Fleck, B., Poland, A.I.: 1995, The SOHO mission: an overview. *Solar Phys.* **162**, 1 – 2. doi:10.1007/BF00733425.

Duvall, T.L., Jr.: 1979, Large-scale solar velocity fields. *Solar Phys.* **63**, 3 – 15. doi:10.1007/BF00155690.

Fox, P., McIntosh, P., Wilson, P.R.: 1998, Coronal holes and the polar field reversals. *Solar Phys.* **177**, 375 – 393.

Gopalswamy, N., Lara, A., Yashiro, S., Howard, R.A.: 2003, Coronal mass ejections and solar polarity reversal. *Astrophys. J. Lett.* **598**, L63 – L66. doi:10.1086/380430.

Haber, D.A., Hindman, B.W., Toomre, J., Bogart, R.S., Larsen, R.M., Hill, F.: 2002, Evolving submerged meridional circulation cells within the upper convection zone revealed by ring-diagram analysis. *Astrophys. J.* **570**, 855 – 864. doi:10.1086/339631.

Hathaway, D.H.: 1996, Doppler measurements of the Sun's meridional flow. *Astrophys. J.* **460**, 1027. doi:10.1086/177029.

Hathaway, D.H., Rightmire, L.: 2010, Variations in the Suns meridional flow over a solar cycle. *Science* **327**, 1350. doi:10.1126/science.1181990.

Hathaway, D.H., Gilman, P.A., Harvey, J.W., Hill, F., Howard, R.F., Jones, H.P., Kasher, J.C., Leibacher, J.W., Pintar, J.A., Simon, G.W.: 1996, GONG observations of solar surface flows. *Science* **272**, 1306 – 1309. doi:10.1126/science.272.5266.1306.

Komm, R.W., Howard, R.F., Harvey, J.W.: 1993, Meridional flow of small photospheric magnetic features. *Solar Phys.* **147**, 207 – 223. doi:10.1007/BF00690713.

Layden, A.C., Fox, P.A., Howard, J.M., Sarajedini, A., Schatten, K.H.: 1991, Dynamo-based scheme for forecasting the magnitude of solar activity cycles. *Solar Phys.* **132**, 1 – 40. doi:10.1007/BF00159127.

Mercier, C., Subramanian, P., Kerdraon, A., Pick, M., Ananthakrishnan, S., Janardhan, P.: 2006, Combining visibilities from the giant meterwave radio telescope and the Nancay radio heliograph. High dynamic range snapshot images of the solar corona at 327 MHz. *Astron. Astrophys.* **447**, 1189 – 1201. doi:10.1051/0004-6361:20053621.

Parker, E.N.: 1955a, Hydromagnetic dynamo models. *Astrophys. J.* **122**, 293. doi:10.1086/146087.

Parker, E.N.: 1955b, The formation of sunspots from the solar toroidal field. *Astrophys. J.* **121**, 491. doi:10.1086/146010.

Schatten, K., Sofia, S.: 1996, Forecasting solar activity and cycle 23 outlook. *Bull. Am. Astron. Soc.* **28**, 1347.

Schatten, K.H., Scherrer, P.H., Svalgaard, L., Wilcox, J.M.: 1978, Using dynamo theory to predict the sunspot number during solar cycle 21. *Geophys. Res. Lett.* **5**, 411 – 414. doi:10.1029/GL005i005p00411.

Scherrer, P.H., Bogart, R.S., Bush, R.I., Hoeksema, J.T., Kosovichev, A.G., Schou, J., Rosenberg, W., Springer, L., Tarbell, T.D., Title, A., Wolfson, C.J., Zayer, I., MDI Engineering Team: 1995, The solar oscillations investigation – Michelson Doppler Imager. *Solar Phys.* **162**, 129 – 188. doi:10.1007/BF00733429.

Steenbeck, M., Krause, F.: 1969, On the dynamo theory of stellar and planetary magnetic fields. I. AC dynamos of solar type. *Astron. Nachr.* **291**, 49 – 84.

Wang, Y., Sheeley, N.R., Jr., Nash, A.G.: 1991, A new solar cycle model including meridional circulation. *Astrophys. J.* **383**, 431 – 442. doi:10.1086/170800.